THE JOURNAL OF PHYSICAL CHEMISTRY B

ARTICLE

pubs.acs.org/JPCB

High-Temperature Vaporization of B_2O_3(l) under Reducing Conditions

Nathan S. Jacobson*

NASA Glenn Research Center, Cleveland, Ohio 44135, United States

Dwight L. Myers

East Central University, Ada, Oklahoma 74820, United States

Supporting Information

ABSTRACT: The vaporization of B_2O_3 in a reducing environment leads to the formation of both B_2O_3(g) and B_2O_2(g). Whereas the formation of B_2O_3(g) is well understood, many questions about the formation of B_2O_2(g) remain. Previous studies using B(s) + B_2O_3(l) have led to inconsistent thermodynamic data. In this study, it was found that, after heating, B(s) and B_2O_3(l) appeared to separate and variations in contact area likely led to the inconsistent vapor pressures of B_2O_2(g). To circumvent this problem, the activity of boron was fixed with a two-phase mixture of FeB and Fe_2B. Both second- and third-law enthalpies of formation were measured for B_2O_2(g) and B_2O_3(g). From these values, the enthalpies of formation at 298.15 K were calculated to be −479.9 ± 25.7 kJ/mol for B_2O_2(g) and −833.4 ± 13.1 kJ/mol for B_2O_3(g). Ab initio calculations to determine the enthalpies of formation of B_2O_2(g) and B_2O_3(g) were conducted using the W1BD composite method and showed good agreement with the experimental values.

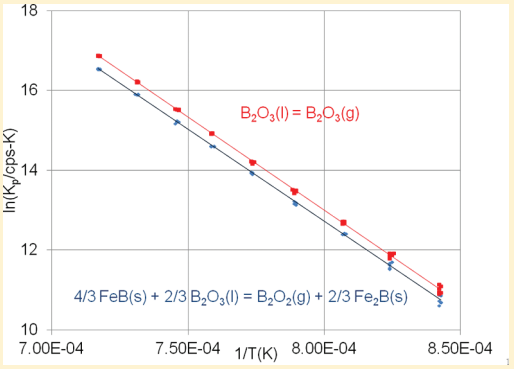

INTRODUCTION

The vaporization of B_2O_3 under reducing conditions is of interest in a variety of applications, such as the degradation of borate-containing re-entry shields. In a controlled thermodynamic study, the most obvious way to attain such conditions is with a mixture of B and B_2O_3. However, an examination of previous experimental studies indicates discrepancies and problems attaining reliable equilibrium data with such a mixture. Inghram et al.[1] first examined mixtures of B and B_2O_3 with a Knudsen effusion mass spectrometer (KEMS) and an alumina Knudsen cell. With B/B_2O_3 molar ratios of >1, they saw signals from both B_2O_3(g) and B_2O_2(g). The dominant reaction in the mixture is

$$\frac{2}{3}B(s) + \frac{2}{3}B_2O_3(l) = B_2O_2(g) \quad (1)$$

They reported an enthalpy of reaction at 1400 K of $\Delta_r H^\circ_{1400}$ = 393.3 ± 33.5 kJ/mol and also calculated an enthalpy of formation of B_2O_2(g). Because signals for both B_2O_2(g) and B_2O_3(g) were observed, the equilibrium reaction between these two vapors was also examined and used to calculate an enthalpy of formation for B_2O_2(g)

$$\frac{2}{3}B(s) + \frac{2}{3}B_2O_3(g) = B_2O_2(g) \quad (2)$$

When Inghram et al.[1] examined pure B_2O_3(l) in an alumina cell, the signal for B_2O_3(g) was about a factor of 5 higher than that for B−B_2O_3 mixtures. They suggested the possibility that the B and B_2O_3 mixtures form a solution with a lower activity of B_2O_3.

Scheer[2] examined mixtures of B and B_2O_3 with a torsion effusion−weight loss technique, utilizing a tantalum effusion cell. He saw B_2O_2(g) as the primary vapor constituent, again indicating that reaction 1 is the dominant reaction. However, he reported an enthalpy of reaction at 1400 K of $\Delta_r H^\circ_{1400}$ = 301.5 kJ/mol, which is significantly different from that reported by Inghram et al.[1] Scheer[2] suggested that this might be due to a sluggish equilibrium, which is often a concern in Knudsen cell studies. Scheer also suggested that the condensed phases might be more complex than simply a B + B_2O_3 mixture and might also include a polymeric solution. B_2O_2(g) can form by either reaction 1 or the sequence

$$\frac{x}{3}B(s) + \frac{x}{3}B_2O_3(l) = (BO)_x(l) \quad (3a)$$

$$(BO)_x(l) = \frac{x}{2}B_2O_2(g) \quad (3b)$$

Other investigators have discussed this issue and obtained data on B_2O_2(g) through other reaction routes. Searcy and Myers[3] examined the reduction of MgO by B to yield Mg(g) and B_2O_2(g). However, they suggested that limited contact area between the solid reactant phases might not have allowed equilibrium to be attained. Rentzepis et al.[4] felt that they avoided the contact issue and the problems associated with B + B_2O_3 by

Received: July 8, 2011
Revised: September 27, 2011
Published: September 29, 2011

   dx.doi.org/10.1021/jp206480d | J. Phys. Chem. B 2011, 115, 13253–13260

using an intimate mixture of carbon and B_2O_3. This creates a large amount of CO(g), but also B_2O_2(g), which was separately condensed and analyzed to obtain vapor pressures.

Despite these issues, data for B_2O_2(g) are listed in both the JANAF[5] and IVTAN[6] compendia. Only the above references are given, and the derived enthalpy of formation for B_2O_2(g) is given a low class of accuracy (6F, ≤40 kJ/mol) in the IVTAN compendium.

In contrast to the formation of B_2O_2(g), the vaporization of B_2O_3 alone to B_2O_3(g) is better understood, and a number of measurements are reported in the literature.[5−9] There is agreement that this process occurs by simple vaporization

$$B_2O_3(l) = B_2O_3(g) \quad (4)$$

The purpose of this article was to explore the B + B_2O_3 system, understand the reasons for the discrepancies, and obtain more reliable thermodynamic data. We started with ab initio calculations of the enthalpies of formation of B_2O_2(g) and B_2O_3(g) for comparison to the experimental values. In the experiments, we paid particular attention to the cell material, attainment of equilibrium in the cell, and analysis of the compounds after heating.

THEORETICAL COMPUTATION OF ENTHALPIES OF FORMATION OF B_2O_2(g) AND B_2O_3(g)

Theoretical calculations of the enthalpies of formation of B_2O_2(g) and B_2O_3(g) were performed using the well-known W1BD[10−14] composite methods. Calculations were performed on the Sooner cluster at the Oklahoma University Supercomputing Center for Education and Research (OSCER), using the Gaussian 09 program, revision B.01.[13] The W1BD method as implemented in Gaussian 09 was used without modification for this study. Input files were created using GaussView 4.1.2.[14] Three different reactions were chosen for comparison's sake to calculate the enthalpies of formation of B_2O_2(g) and B_2O_3(g). Note that all molecules are in the singlet spin state unless otherwise indicated.

$$B_2O_2(g) = 2B(g, \text{doublet}) + 2O(g, \text{triplet}) \quad (5)$$

$$B_2O_2(g) + 6HF(g) = 2BF_3(g) + 2H_2O(g) + H_2(g) \quad (6)$$

$$B_2O_2(g) + 6H_2(g) = 2BH_3(g) + 2H_2O(g) + H_2(g) \quad (7)$$

$$B_2O_3(g) = 2B(g, \text{doublet}) + 3O(g, \text{triplet}) \quad (8)$$

$$B_2O_3(g) + 6HF(g) = 2BF_3(g) + 3H_2O(g) \quad (9)$$

$$B_2O_3(g) + 6H_2(g) = 2BH_3(g) + 3H_2O(g) \quad (10)$$

Reactions 5 and 8 were chosen because of the common use of atomization reactions for computing standard enthalpies. Reactions 6, 7, 9, and 10 were chosen because they are isogyric reactions. Thermodynamic data for all species except, of course, B_2O_2(g) and B_2O_3(g) were taken from the JANAF tables.[5]

The protocol for W1 theory was detailed by Martin and coworkers.[10,11] The essential elements of the method are given here. The method makes use of density functional theory at the B3LYP/VTZ+1 level to determine equilibrium geometries and harmonic frequencies, which are scaled by 0.985 to obtain the zero-point energy. Single-point calculations are carried out using CCSD(T)/AVDZ+2d, CCSD(T)/AVTZ+2d1f, and CCSD/AVQZ+2d1f, where the notation AV*n*Z is shorthand for the aug-cc-pV*n*z basis sets, with n = D, T, or Q. The self-consistent-field (SCF) component of the total atomization energy is extrapolated by the function $A + B/C^l$ from the SCF/AVDZ+2d, SCF/AVTZ+2d1f, and SCF/AVQZ+2d1f components of the total atomization energy, with l = 2, 3, and 4, respectively. The value of the β parameter is set to 3.22, and the CCSD valence correlation component is obtained from the function $A + B/l^\beta$ as applied to CCSD/AVTZ+2d1f and CCSD/AVQZ+2d1f valence correlation energies, with l = 3 and 4, respectively. The (T) valence correlation component is determined by applying the same formula to CCSD(T)/AVDZ+2d and CCSD(T)/AVTZ+2d1f values for the (T) contribution. Core correlations are obtained using a reduced basis set using CCSD(T). Relativistic corrections are introduced for improved accuracy in all W1 variants. Scalar relativistic and spin−orbit coupling effects are treated using a reduced basis set with an averaged coupled pair functional (ACPF). The W1BD[12] method differs from the W1 protocol in that it incorporates the Brueckner doubles variant of coupled-cluster theory to simplify computations.

A summary of the experimental determinations of the structures of B_2O_2(g) and B_2O_3(g) can be found in the JANAF tables.[5] The best evidence supports a linear O−B−B−O shape for B_2O_2(g)[15−17] and a V-shaped structure for B_2O_3(g).[15−19] For this study, the geometry was set to $D_{\infty h}$ for B_2O_2 and C_{2v} for B_2O_3. From the W1BD calculations, the bond distances for B_2O_2 are r(B−B) = 1.6357 Å and r(B−O) = 1.1991 Å. For B_2O_3 (C_{2v} symmetry), the bond distances are r(B−O) = 1.3238 Å for the central O atom and r(B−O) = 1.207 Å for the extremal O atoms. Bond angles are ∠B−O−B = 144.1061° and ∠O−B−O = 182.2946°. Frequencies are listed in Table 1 for both species.

Table 1. Frequencies (cm^{-1}) Computed at the cc-pVTZ+d (5d,7f) Level for B_2O_2 and B_2O_3[a]

B_2O_2	B_2O_3	
215 (Π_u)	88 (A_1)	736 (A_1)
496 (Π_g)	466 (B_2)	1264 (B_2)
612 (Σ_g)	472 (A_2)	2112 (A_1)
1960 (Σ_u)	491 (B_1)	2113 (B_2)
2125 (Σ_g)	526 (A_1)	

[a] (5d,7f) notation indicates the use of pure d and f functions rather than Cartesian functions.[20]

Table 2 provides a complete summary of all W1BD energy terms computed for B_2O_2(g) and B_2O_3(g). Table 1 in the Supporting Information lists the W1BD enthalpies computed for all species used in this study.

The computed enthalpies of formation can be seen in Table 3. The enthalpies based on reactions 7 and 10 are in agreement with those based on reactions 5 and 6 and reactions 8 and 9, respectively, within experimental uncertainties of the species employed for these reactions. Of the reactions used, reactions 6 and 9 use species with the least uncertainties in their experimental enthalpies according to the JANAF tables.[5] The results from the W1BD theory calculations for reactions 6 and 9 should therefore be the most reliable theoretical values from this study for enthalpies of formation of B_2O_3(g) and B_2O_2(g).

Table 2. Summary of All W1BD Terms for $B_2O_3(g)$ and $B_2O_2(g)$ Used in Calculation of Enthalpies of Formation[a,b]

	$B_2O_3(g)$			$B_2O_2(g)$		
	reference	BD	BD(T)	reference	BD	BD(T)
AVDZ+2d	−274.150900	−274.883460	−274.911721	−199.195803	−199.748363	−199.772783
AVTZ+2df	−274.227080	−275.104412	−275.145592	−199.244428	−199.899786	−199.934083
AVQZ+2df	−274.246961	−275.175489		−199.258688	−199.949899	
	NR/FC	DKH/full		NR/FC	DKH/full	
MTsmall	−275.166592	−275.596836		−199.950834	−200.273488	
	reference	BD	BD(T)	reference	BD	BD(T)
extrapolated energy components	−274.253147	−0.962095	−0.045982	−199.263124	−0.714717	−0.037968
core + scalar relativistic component	−0.430245			−0.322654		
W1BD electronic energy	−275.691468			−200.338464		
E(ZPE)	0.018555			0.013734		
W1BD (0 K)	−275.672913			−200.324730		
W1BD enthalpy (298.15 K)	−275.667303			−200.319715		
E(thermal)	0.023222			0.017805		
W1BD energy (298.15 K)	−275.668247			−200.320659		
W1BD free energy (298.15 K)	−275.699748			−200.347865		

[a] All energies in hartrees, pressure = 1 atm. [b] BD = Brueckner doubles, BD(T) = Brueckner doubles with approximate triples, NR/FC = nonrelativistic, frozen core, DKH = Douglas−Kroll−Hess relativistic electrons-only method, MTsmall = Martin−Taylor small correlation basis sets.

Table 3. Summary of Calculated Enthalpies of Formation by Reaction and Composite Method

reaction	W1BD enthalpy (kJ mol^{-1})	Nguyen et al.[21] enthalpy (kJ mol^{-1})
	$B_2O_2(g)$	
(5) $B_2O_2(g) = 2B(g, doublet) + 2O(g, triplet)$	−479.9 ± 17.2	−457.7
(6) $B_2O_2(g) + 6HF(g) = 2BF_3(g) + 2H_2O(g) + H_2(g)$	−456.7 ± 5.3	
(7) $B_2O_2(g) + 6H_2(g) = 2BH_3(g) + 2H_2O(g) + H_2(g)$	−441.1 ± 14.7	
	$B_2O_3(g)$	
(8) $B_2O_3(g) = 2B(g, doublet) + 3O(g, triplet)$	−857.4 ± 17.2	−830.1
(9) $B_2O_3(g) + 6HF(g) = 2BF_3(g) + 3H_2O(g)$	−831.8 ± 5.3	
(10) $B_2O_3(g) + 6H_2(g) = 2BH_3(g) + 3H_2O(g)$	−816.2 ± 14.8	

Nguyen et al.[21] examined many boron−oxygen species using a similar ab initio approach. Their results for B_2O_2 and B_2O_3 (based on reactions 5 and 8) are also included in Table 3. There is close agreement between their results and our W1BD results taken from reactions 6 and 9. There is less agreement between our results and theirs for our reactions 5 and 8. In general, one would expect the values based on an isogyric reaction to be more reliable than those based on a reaction where total spin multiplicity is not conserved.

EXPERIMENTAL SECTION

Boron nitride (BN) was selected as the cell material. Oxidation studies of BN indicate a B_2O_3 film forms on the BN substrate, showing that BN is stable in the presence of B_2O_3.[22] Three systems were studied: B_2O_3 (99.9% pure, Alfa-Aesar, Ward Hill, NY) in a BN (99% pure, grade AX-05, St. Gobain, Amherst, NY) cell, B (99% pure, Alfa-Aesar, Ward Hill, NY) + B_2O_3 in a 1:1 molar mixture in a BN cell, and FeB (98% pure, Alfa-Aesar, Ward Hill, NY) + Fe_2B (98% pure, Alfa-Aesar, Ward-Hill, NY) + B_2O_3 in a 1:1:1 molar mixture in a BN cell. Micron-sized powders were mixed with a mortar and pestle and placed in a BN cell with 1.5-mm-diameter orifice.

Vapor pressure measurements were made using a modified Nuclide-type 12-HT-90 Knudsen effusion mass spectrometer. The details of this instrument have been described elsewhere.[23] A single Knudsen cell furnace was used. The Knudsen cell was resistively heated with a tantalum element in a "hairpin" shape.[23] After exposure to the B−O vapors, the element discolored somewhat because of some type of interaction with the vapors; however, it held its rigid shape and heating characteristics. Temperatures were measured with a disappearing-filament-type pyrometer (Pyro Microtherm, Windsor, NJ), calibrated against the melting point of gold in a graphite crucible. Electron-impact ionization was used, and ions were extracted mutually perpendicular to the molecular and electron beams. Ions were sorted with a magnetic sector, and signal intensity was determined by ion counting.

The calibration constant was determined from the relationship of the ion intensity to the partial pressure of the

Table 4. Measured Appearance Energies of the Ions in the Mass Spectra of the Vapor over B_2O_3 + Fe_2B + FeB

	appearance energy	
ion	Inghram et al.[1]	this study
B^+	15.7	14.8
BO^+	18.8	18.4
$B_2O_2^+$	13	13.0
$B_2O_3^+$	13.2	13.0

Table 5. Mass Spectra of the Vapor Species over B_2O_3 and Fe_2B + FeB + B_2O_3 in the BN Cell

ion	B_2O_3, 1300 K	Fe_2B + FeB + B_2O_3, 1350 K
B^+	0.02	0.19
BO^+	0.07	0.07
$B_2O_2^+$	0.11	0.73
$B_2O_3^+$	1.00	1.00

vapor species[23,24]

$$P(i) = \frac{kI(i)T}{\sigma(E)} \tag{11}$$

where $P(i)$ is the partial pressure of a species i in the Knudsen cell in bar, k is the calibration constant in bar·m^2/cps·K, $I(i)$ is the ion intensity of the parent ion of species i in counts per second (cps), T is the absolute temperature in Kelvin, and $\sigma(E)$ is the ionization cross section in m^2. For species with appreciable amounts of isotopes, such as B, corrections for isotopic abundances must also be made. The calibration constant, k, was determined from the triple-point plateau of Au at 1337.3 K.

Appearance energies of each ion were measured using the linear extrapolation method. Values read from the instrument were corrected from measurements on gold, whose tabulated appearance energy was taken as 8.9 eV.[25] The measured appearance energies are listed in Table 4.

It should be noted that these values are only approximate, with estimated errors of ±0.5 eV. They were taken only to establish a working ionization energy for this study. On the basis of these data, a working ionization energy of 26.2 eV was selected for this study. It is known that pure B_2O_3(l) vaporizes primarily to B_2O_3(g),[1] and as shown in Table 5, $B_2O_3^+$ ions were attributable to B_2O_3(g). The addition of a reducing agent, such as FeB/Fe_2B, also forms B_2O_2(g). Thus, as shown, in Table 5, $B_2O_2^+$ ions were primarily attributable to B_2O_2(g). The lower intensities of B^+ and BO^+ and their higher appearance energies indicate these species are formed through ionization and dissociation, as suggested by Inghram et al.[1]

Ionization cross sections for Au and the B−O species were calculated using the Deutsch-Mark method[26−28] in conjunction with the GAMESS code.[29] Geometry optimizations were performed at the MP2/6-311G level of theory for both molecules, and Mulliken population analysis was used in the Deutsch-Mark formalism. Table 6 lists the cross sections used in the calculations. For comparison, we list cross sections calculated by conventional methods,[30] the additivity rule[24] for molecules, and adjusted to 26 eV.[31] The latter was done by fitting Mann's cross-section calculations[30] to the Bell-type function.[32]

Each peak was scanned six times to give six data points at each temperature. Each individual point was included in a van't Hoff

Table 6. Ionization Cross Sections of Vapor Species Calculated at 26 eV

	cross section (×10^{-20} m^2)	
species	Deutsch-Mark	Mann and additivity rule
Au	4.84	5.49
B_2O_2(g)	7.19	4.77
B_2O_3(g)	7.63	5.34

plot of $\ln[I(i)T]$ versus $1/T$. Second-law enthalpies were obtained using the usual methods,[33] taking the slope of the van't Hoff plot and obtaining an enthalpy of reaction, $\Delta_r H_T^\circ$, from

$$\frac{\mathrm{d}\ln[I(i)T]}{\mathrm{d}\left(\frac{1}{T}\right)} = -\frac{\Delta_r H_T^\circ(i)}{R} \tag{12}$$

where R is the gas constant and $\Delta_r H_T^\circ(i)$ is the reaction enthalpy at the average measurement temperature, T. To obtain the enthalpy at 298 K, the sigma-plot method was used[34,35]

$$\Delta[-(\mathrm{gef}_{298.15})] - R\ln[I(i)T] = A + B/T \tag{13}$$

where the Gibbs free energy function is given by $\mathrm{gef}_{298.15} = (G_T^\circ - H_{298.15}^\circ)/T$ for each phase with G_T° equal to the Gibbs energy and $H_{298.15}^\circ$ equal to the enthalpy. The Gibbs free energy functions were taken from ref 5. Because these function were determined from experimental spectroscopic methods, they are preferred over the theoretical calculations. Plotting the left-hand side of eq 13 versus $1/T$, the slope (B) gives $\Delta_r H_{298.15}^\circ$ at 298.15 K.

Third-law enthalpies were also obtained using the usual methods. Pressures were obtained from eq 11, using the calibration constant derived from the triple point of Au and ionization cross sections of the vapor species calculated as described in the Experimental Section. Corrections were made for the isotopes of boron. These were put into the standard third-law expression

$$T\{\Delta[-(\mathrm{gef}_{298.15})] - R\ln(K)\} = \Delta_r H_{298.15}^\circ \tag{14}$$

where $\mathrm{gef}_{298.15}$ was defined previously and K is the equilibrium constant for the reaction under examination. In a third-law analysis, enthalpies are calculated for each data point, and the average is determined.

In all cases, the measured enthalpy of reaction was used to calculate an enthalpy of formation at 298.15 K for B_2O_2(g) and B_2O_3(g). The enthalpy of formation of B_2O_3(l) at 298.15 K, −1253.359 ± 2.51 kJ/mol, was taken from the JANAF tables.[5] Enthalpies of formation at 298.15 K of other borides were necessary to derive the B_2O_2(g) enthalpy of formation at 298.15 K and will be discussed in the next section.

RESULTS AND DISCUSSION

Initial experiments were conducted with a B + B_2O_3 mixture, as used by Inghram et al.[1] and Scheer.[2] However, even after long equilibration times (>1 h at each temperature), it was not possible to obtain reproducible data. After taking a measurement at one temperature followed by other measurements at different temperatures, new measurements at the first temperature gave significantly different ion intensities. An examination of the cell contents after a run indicated a clear macroscopic separation between the boron particles and solidified B_2O_3 liquid, as shown

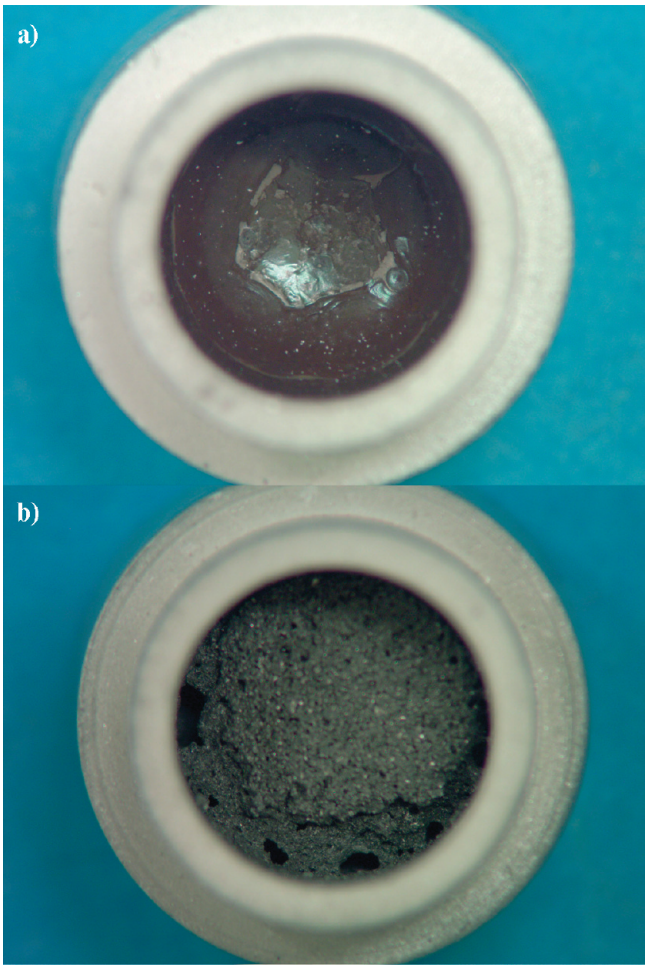

Figure 1. Appearance of solids in the BN cell after heating: (a) 1:1 molar mixture of B and B_2O_3 that was well-mixed before heating. After heating, it shows a clear, glassy material in the center, which is the solidified B_2O_3, with B forming a bowl on the outside. (b) 1:1:1 molar mixture of FeB + Fe_2B + B_2O_3. Intimate mixing is retained after heating.

in Figure 1a. Further tests with a larger ~3-mm piece of boron suggested that the B_2O_3 liquid did not wet the boron and that insufficient contact area was attained for proper equilibration. We believe that this is the explanation for the inconsistent data in the literature[1,2] and the problems with B + B_2O_3 mixtures discussed by Rentzepis et al.[4]

To circumvent this problem and still provide a fixed activity of boron to produce B_2O_2(g), we used a two-phase mixture of Fe_2B and FeB. The Fe−B diagram[36] indicates that this mixture is stable to 1662 K. A mixture of FeB + Fe_2B + B_2O_3 gave reproducible ion intensities; specifically, after taking a measurement at one temperature followed by other measurements at different temperatures, new measurements at the first temperature gave the same ion intensity within a few percent. Further, macroscopically, the mixture appeared to retain intimate mixing after a run, as shown in Figure 1b.

Thus, the reaction measured with the Fe_2B + FeB + B_2O_3 mixture is

$$\frac{4}{3}\mathrm{FeB(s)} + \frac{2}{3}\mathrm{B_2O_3(l)} = \mathrm{B_2O_2(g)} + \frac{2}{3}\mathrm{Fe_2B(s)} \qquad (15)$$

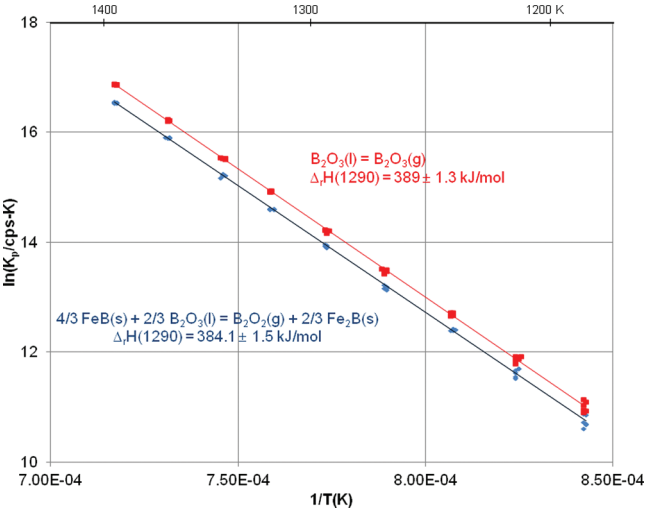

Figure 2. van't Hoff plot for $B_2O_2^+$ and $B_2O_3^+$. The upper line is a plot of $\ln(K_{15})$ versus $1/T$, and the lower line is a plot of $\ln(K_4)$ versus $1/T$.

The equilibrium constant for this reaction is

$$K_{15} = P(\mathrm{B_2O_2}) \propto I(\mathrm{B_2O_2^+})T \qquad (16)$$

The analogue to reaction 2 can be written as

$$\frac{4}{3}\mathrm{FeB(s)} + \frac{2}{3}\mathrm{B_2O_3(g)} = \mathrm{B_2O_2(g)} + \frac{2}{3}\mathrm{Fe_2B(s)} \qquad (17)$$

The equilibrium constant for this reaction is

$$K_{17} = \frac{P(\mathrm{B_2O_2})}{[P(\mathrm{B_2O_3})]^{0.67}} \propto \frac{I(\mathrm{B_2O_2^+})T}{[I(\mathrm{B_2O_3^+})T]^{0.67}} \qquad (18)$$

The congruent vaporization of B_2O_3(l) occurs according to eq 4, and that equilibrium constant is given by

$$K_4 = P(\mathrm{B_2O_3}) \propto I(\mathrm{B_2O_3^+})T \qquad (19)$$

To generate a van't Hoff plot, measurements were made in a random sequence of temperatures from ~1200 to 1400 K, which yielded consistent results, as shown by the straight line Figure 2. The thermodynamic data for FeB and Fe_2B were taken from the Barin compendium.[37]

Three separate runs were conducted, obtaining enthalpies of reaction, $\Delta_r H(T)$, for reactions 15, 17, and 4. These data are summarized in Table 7 and compared to those from other investigators. In all cases, the tabulated Gibbs free energy functions ($\mathrm{gef}_{298.15}$) from the JANAF tables[5] were used. Data points were taken from the other investigations and reanalyzed with these functions.

Our enthalpies for B_2O_2(g) are slightly lower than those reported by other investigators. However, as noted, there were problems in the previous investigations when elemental B was used. Also, container interactions might have been an issue in previous investigations. Both our second- and third-law-derived enthalpies of formation are reasonably close to those in the tables, particularly given the high level of uncertainty assigned to the IVTAN data. Taking the average of the six second-law enthalpies and six third-law enthalpies yields a value of −479.9 ± 8.1 kJ/mol for the enthalpy of formation. Sources of error include the ion intensity measurement (a few percent) and the uncertainty in the temperature measurement (±1K). The major

Table 7. Summary of Our Data and Literature Data for Enthalpies of Reaction and Formation for $B_2O_2(g)$

			enthalpy of reaction			$2B(s) + O_2(g) = B_2O_2(g)$		
investigator and technique	no. of data points	average temperature (K)	from second law $\Delta_r H^\circ_T$ (kJ/mol)	from second law $\Delta_r H^\circ_{298.15}$ (kJ/mol)	from third law $\Delta_r H^\circ_{298.15}$ (kJ/mol)	from second law $\Delta_f H^\circ_{298.15}$ (kJ/mol)	from third law $\Delta_f H^\circ_{298.15}$ (kJ/mol)	tables
Inghram et al.,[1] KEMS	6	1400	302.5 ± 4.2	407.0 ± 7.2	391.5 ± 0.7[a]	−509.4	−444.1	
$^2/_3B(s) + {}^2/_3B_2O_3(l) = B_2O_2(g)$								
Inghram et al.,[1] KEMS	3	1410	103.4 ± 1.0	104.9 ± 1.1	101.4 ± 0.3	−455.2	−458.7	
$^2/_3B(s) + {}^2/_3B_2O_3(g) = B_2O_2(g)$								
Scheer,[2] torsion	14	1390	382.5 ± 7.2	326.2 ± 4.4	372.7 ± 2.0	−428.6	−462.9	
$^2/_3B(s) + {}^2/_3B_2O_3(l) = B_2O_2(g)$								
Rentzepis et al.,[4] collection	5						−466.2 ± 6.5	
$B_2O_3(l) + 3C(s) = 3CO(g) + 2B(s)$								
$B_2O_3(l) + C(s) = B_2O_2(g) + CO(g)$								
Searcy and Myers[3]	1	1375					−458.9 ± 16.7	
$2MgO + 2B = 2Mg(g) + B_2O_2(g)$								
JANAF[5]								−456.1 ± 8.4
IVTAN[6]								−457.728 ± 40
this study, run 1	8	1284	363.8 ± 2.8	384.9 ± 2.9	411.6 ± 1.6	−498.0	−471.4	
$^4/_3FeB(s) + {}^2/_3B_2O_3(l) = B_2O_2(g) + {}^2/_3 Fe_2B(s)$								
this study, run 1	8	1284	113.0 ± 2.1	115.6 ± 2.1	125.1 ± 0.8	−489.2	−479.7	
$^4/_3FeB(s) + {}^2/_3B_2O_3(g) = B_2O_2(g) + {}^2/_3Fe_2B(s)$								
this study, run 2	6	1280	376.7 ± 1.4	399.0 ± 1.5	413.0 ± 0.9	−484.0	−470.0	
$^4/_3FeB(s) + {}^2/_3B_2O_3(l) = B_2O_2(g) + {}^2/_3Fe_2B(s)$								
this study, run 2	6	1280	122.9 ± 1.8	125.6 ± 1.8	125.8 ± 0.5	−479.2	−479.0	
$^4/_3FeB(s) + {}^2/_3B_2O_3(g) = B_2O_2(g) + {}^2/_3Fe_2B(s)$								
this study, run 3	9	1290	384.0 ± 1.5	405.5 ± 1.5	414.0 ± 0.7	−477.5	−469.0	
$^4/_3FeB(s) + {}^2/_3B_2O_3(l) = B_2O_2(g) + {}^2/_3Fe_2B(s)$								
this study, run 3	9	1290	123.6 ± 1.7	123.7 ± 1.7	126.2 ± 0.6	−481.1	−478.6	
$^4/_3FeB(s) + {}^2/_3B_2O_3(g) = B_2O_2(g) + {}^2/_3Fe_2B(s)$								

[a] Inghram et al. converted only three points to pressure, and hence, only three points were used for the third-law enthalpy.

dx.doi.org/10.1021/jp206480d | J. Phys. Chem. B 2011, 115, 13253–13260

Table 8. Summary of Our Data and Literature Data for Enthalpies of Reaction and Formation for $B_2O_3(g)$

			$B_2O_3(l) = B_2O_3(g)$			$2B(s) + {}^3/_2O_2(g) = B_2O_3(g)$		
investigator and technique	no. of data points	average temperature (K)	from second law $\Delta_r H^\circ_T$ (kJ/mol)	from second law $\Delta_r H^\circ_{298.15}$ (kJ/mol)	from third law $\Delta_r H^\circ_{298.15}$ (kJ/mol)	from second law $\Delta_f H^\circ_{298.15}$ (kJ/mol)	from third law $\Delta_f H^\circ_{298.15}$ (kJ/mol)	tables
Hildenbrand,[8] torsion			302.5 ± 4.2	427.5	417.3	−825.9	−836.0	
Scheer,[7] torsion	14	1500	364.9 ± 3.8	405.2 ± 3.9	424.2 ± 0.9	−848.2	−829.2	
Shultz et al.,[9] mass spectrometry and weight loss	14			412.1 ± 8.4	415.5 ± 0.1			
JANAF[5]								−836.0 ± 4.2
IVTAN[6]								−835.383 ± 40
this study B_2O_3 only	11	1320	380.8 ± 1.2	410.7 ± 1.3	429.5 ± 1.2	−842.6	−823.9	
this study, run 1 FeB/Fe_2B/B_2O_3	8	1270	373.2 ± 1.7	401.7 ± 1.8	428.7 ± 1.7	−851.7	−824.7	
this study, run 2 FeB/Fe_2B/B_2O_3	6	1225	380.8 ± 1.7	409.9 ± 1.7	430.3 ± 1.3	−843.5	−823.1	
this study, run 3 FeB/Fe_2B/B_2O_3	9	1290	389.0 ± 1.3	417.9 ± 1.3	430.9 ± 0.8	−835.5	−822.5	

source of uncertainty is the tabulated thermodynamic data for FeB and Fe_2B. As indicated, these data are from the Barin thermochemical tables.[37] The enthalpies of formation used to develop the tables for FeB and Fe_2B are from the calorimetric measurements of Gorelkin et al.,[38,39] who reported $\Delta_f H^\circ_{298}$ values of 71.1 ± 12.5 and 66.9 ± 20.9 kJ/mol for FeB and Fe_2B, respectively. Thus, the uncertainty in our determination of $\Delta_f H^\circ_{298}(B_2O_2)$ must include these uncertainties and be reported as ±25.7 kJ/mol. Our measured enthalpies of formation for $B_2O_2(g)$ is well within the uncertainty of the W1BD calculations in Table 3.

As noted, these runs gave a strong signal for $B_2O_3(g)$ as well. There is some discussion in the literature about the possibility of a solution of B and B_2O_3. However, the ion intensities from the FeB + Fe_2B + B_2O_3 mixtures in our measurements were the same as those from the B_2O_3 alone, indicating this did not occur. As shown in Table 8, our enthalpies were virtually the same. We compare our data to selected literature data. More literature data are given in the JANAF tables.[5] Again, there is some discrepancy between the second- and third-law measurements. We take the average of the three second-law measurements and three third-law measurements to obtain a enthalpy of formation of −833.4 ± 13.1 kJ/mol for $B_2O_3(g)$. This is also well within the uncertainty of the W1BD calculations in Table 3.

CONCLUSIONS

The vaporization of B_2O_3 in reducing atmospheres has been studied. Previous issues with B + B_2O_3 were explained by an observed phase separation and inadequate reactive contact area. To fix an activity of B, a two-phase FeB + Fe_2B mixture was used. This gave reproducible data for $B_2O_2(g)$ vapor pressures. Enthalpies of reaction were calculated for the FeB−$B_2O_3(l)$/Fe_2B−$B_2O_2(g)$, FeB−$B_2O_3(g)$/Fe_2B−$B_2O_2(g)$, and $B_2O_3(l)$/$B_2O_3(g)$ equilibria. From replicate measurements of each using both second- and third-law methods, the following enthalpies of formation were derived: −479.9 ± 25.7 kJ/mol for $B_2O_2(g)$ and −833.4 ± 13.1 kJ/mol for $B_2O_3(g)$. Error analysis indicated that the major source of error is uncertainty in the enthalpies of formation for FeB and Fe_2B. The measured enthalpies of formation for $B_2O_2(g)$ and $B_2O_3(g)$ are in good agreement with the ab initio W1BD calculations.

ASSOCIATED CONTENT

Supporting Information. Summary of W1BD enthalpies for all species used in reactions 5−10, computed enthalpies of formation and measured ion intensities. This material is available free of charge via the Internet at http://pubs.acs.org.

AUTHOR INFORMATION

Corresponding Author

*E-mail: nathan.s.jacobson@nasa.gov.

ACKNOWLEDGMENT

OSCER (University of Oklahoma) Dr. Henry Neeman, Director; Sr. Systems Analyst David Akin; and Joshua Alexander, HPC Application Software Specialist, provided valuable technical expertise. We also thank Dr. C. Rice and Mr. J. Halye, Department of Chemistry and Biochemistry, University of Oklahoma, Norman, OK, for access to Gaussian and assistance with the calculations. Helpful discussions with Dr. E. Copland, ATI Allvac, Monroe, NC, are very much appreciated. We are also grateful to Dr. V. Stolyarova, St. Petersburg State University, St. Petersburg, Russia, for many helpful comments on the manuscript.

REFERENCES

(1) Inghram, M. G.; Porter, R. F.; Chupka, W. A. *J. Chem. Phys.* **1956**, *25*, 498–501.
(2) Scheer, M. D. *J. Phys. Chem.* **1958**, *62*, 490–498.
(3) Searcy, A. W.; Myers, C. E. *J. Phys. Chem.* **1957**, *61*, 957–960.
(4) Rentzepis, P.; White, D.; Walsh, P. N. *J. Phys. Chem.* **1960**, *64*, 1784–1787.

(5) Chase, M. W. *NIST−JANAF Thermochemical Tables*, 4th ed.; Journal of Physical and Chemical Reference Data Monograph 9; American Chemical Society: Washington, DC, 1998.
(6) Gurvich, L. V.; Veyts, I. V., Alcock, C. B. Eds. *Thermodynamic Properties of Individual Substances*, 4th ed.; Begell House: New York, 1989.
(7) Scheer, M. D. *J. Phys. Chem.* **1957**, *61*, 1184–1188.
(8) Hildenbrand, D. L.; Hall, W. F.; Potter, N. D. *J. Chem. Phys.* **1963**, *39*, 296–301.
(9) Shultz, M. M.; V.L. Stolyarova, V. L.; Semenov, G. A. *Fiz. Khim. Stekla* **1978**, *4*, 653–660.
(10) Martin, J. M. L.; de Oliveira, G. *J. Chem. Phys.* **1999**, *111*, 1843–1856.
(11) Parthiban, S.; Martin, J. M. L. *J. Chem. Phys.* **2001**, *114*, 6014–6029.
(12) Kobayashi, R.; Handy, N. C.; Amos, R. D.; Trucks, G. W.; Frisch, M. J.; Pople, J. A. *J. Chem. Phys.* **1991**, *95*, 6723–6733.
(13) Frisch, M. J.; Trucks, G. W.; Schlegel, H. B.; Scuseria, G. E.; Robb, M. A.; Cheeseman, J. R.; Scalmani, G.; Barone, V.; Mennucci, B.; Petersson, G. A.; Nakatsuji, H.; Caricato, M.; Li, X.; Hratchian, H. P.; Izmaylov, A. F.; Bloino, J.; Zheng, G.; Sonnenberg, J. L.; Hada, M.; Ehara, M.; Toyota, K.; Fukuda, R.; Hasegawa, J.; Ishida, M.; Nakajima, T.; Honda, Y.; Kitao, O.; Nakai, H.; Vreven, T.; Montgomery, J. A., Jr.; Peralta, J. E.; Ogliaro, F.; Bearpark, M.; Heyd, J. J.; Brothers, E.; Kudin, K. N.; Staroverov, V. N.; Kobayashi, R.; Normand, J.; Raghavachari, K.; Rendell, A.; Burant, J. C.; Iyengar, S. S.; Tomasi, J.; Cossi, M.; Rega, N.; Millam, J. M.; Klene, M.; Knox, J. E.; Cross, J. B.; Bakken, V.; Adamo, C; Jaramillo, J.; Gomperts, R. E.; Stratmann, O.; Yazyev, A. J.; Austin, R.; Cammi, C.; Pomelli, J. W.; Ochterski, R.; Martin, R. L.; Morokuma, K.; Zakrzewski, V. G.; Voth, G. A.; Salvador, P.; Dannenberg, J. J.; Dapprich, S.; Daniels, A. D.; Farkas, O.; Foresman, J. B.; Ortiz, J. V.; Cioslowski, J.; Fox, D. J. *Gaussian 09*, revision B.01; Gaussian Inc.: Wallingford, CT, 2009
(14) GaussView 5 Features at a Glance. http://www.gaussian.com/g_prod/gv_glance.htm (accessed June 2011).
(15) Weltner, J. W.; Warn, J. R.W. *J. Chem. Phys.* **1962**, *37*, 292–303.
(16) Sommer, A.; White, D.; Linevsky, M. J.; Mann, D. E. *J. Chem. Phys.* **1963**, *38*, 87–98.
(17) Burkholder, T. R.; Andrews, L. *J. Chem. Phys.* **1991**, *95*, 8697–8709.
(18) Akishin, P. A.; Spiridonov, V. P. *Dokl. Akad. Nauk SSSR* **1960**, *131*, 557–560.
(19) Kaiser, E. W.; Muenter, J. S.; Klemperer, W. *J. Chem. Phys.* **1968**, *48*, 3339.
(20) Frisch, A.; Frisch, M. J.; Clemente, F. R.; Trucks, G. W. *Gaussian 09 User's Reference*; Gaussian, Inc., Wallingford, CT, 2009.
(21) Nguyen, M. T.; Matus, M. H.; Vu, T. N.; Grant, D. J.; Dixon, D. A. *J. Phys. Chem. A* **2009**, *113*, 4895–4909.
(22) Jacobson, N.; Farmer, S.; Moore, A.; Sayir, H. *J. Am. Ceram. Soc.* **1999**, *82*, 393–398.
(23) Copland, E. H.; Jacobson, N. S. *Measuring Thermodynamic Properties of Metals and Alloys with Knudsen Effusion Mass Spectrometry*; NASA Technical Paper TP—2010-216795; National Aeronautics and Space Administration (NASA): Springfield, VA, 2010.
(24) Hilpert, K. *Rapid Commun. Mass Spectrom.* **1991**, *5*, 175–187.
(25) Levin, R. D.; Lias, S. G. *Ionization Potential and Appearance Potential Measurements, 1971−1981*; National Bureau of Standards: Washington, DC, 1982. Available at http://purl.access.gpo.gov/GPO/LPS113176.
(26) Deutsch, H.; Becker, K.; Mark, T. D. *Int. J. Mass Spectrom.* **2008**, *271*, 58–62.
(27) Margreiter, D.; Deutsch, H.; Mark, T. D. *Int. J. Mass Spectrom. Ion Processes* **1994**, *139*, 127–139.
(28) Deutsch, H.; Scheier, P.; Matt-Leubner, S.; Becker, K.; Mark, T. D. *Int. J. Mass Spectrom.* **2005**, *243*, 215–221.
(29) Schmidt, M. W.; Baldridge, K. K.; Boatz, J. A.; Elbert, S. T.; Gordon, M. S.; Jensen, J. H.; Koseki, S.; Matsunaga, N.; Nguyen, K. A.; Su, S.; Windus, T. L.; Dupuis, M.; Montgomery, J. A. *J. Comput. Chem.* **1993**, *14*, 1347–1363.
(30) Mann, J. B. *J. Chem. Phys.* **1967**, *46*, 1646–1651.
(31) Bonnell, D. W. *SIGMA* , version 1.1; National Institute of Standards and Technology (NIST): Gaithersburg, MD, 1990
(32) Bell, K. L.; Gilbody, H. B.; Hughes, J. G.; Kingston, A. E.; Smith, F. J. *J. Phys. Chem. Ref. Data* **1983**, *12*, 891–916.
(33) Drowart, J.; Goldfinger, P. *Angew. Chem., Int. Ed. Engl.* **1967**, *6*, 581–648.
(34) Cubicciotti, D. *J. Phys. Chem.* **1966**, *70*, 2410–2413.
(35) Copland, E. H. *Long Term Measurement of the Vapor Pressure of Gold in the Au−C System*; NASA Contractor Report NASA/CR—2009-215498; National Aeronautics and Space Administration (NASA): Springfield, VA, 2009.
(36) Massalski, T. B.; Okamoto, H. *Binary Alloy Phase Diagrams*; ASM International: Metals Park, OH, 1990.
(37) Barin, I. *Thermochemical Data of Pure Substances*, 3rd ed.; VCH: Weinheim, Germany, 1995.
(38) Kubachewski, O.; Alcock, C. B. *Metallurgical Thermochemistry*, 5th ed.; Pergamon Press: Oxford, U.K., 1979.
(39) Gorelkin, O. S.; Chirkov, N. A.; Kolesnik., O.; Dubrovin, A. S. *Russ. J. Phys. Chem. USSR* **1972**, *46*, 431–432.